Periodica Polytechnica
Mechanical Engineering

Frequency and Phase Characteristics of the Edge Tone Part II.

58(1), pp. 69-76, 2014
DOI:10.3311/PPme.7031

István Vaik, Roxána Varga, György Paál

RESEARCH ARTICLE

RECEIVED 3 SEPTEMBER 2013

Abstract

This paper is the second half of a two-part publication. The first part contains a detailed overview of the edge tone literature and also describes the qualitative behaviour of the edge tone when varying its main parameters i.e. the mean exit velocity of the jet and the nozzle-to-wedge distance in the case of both top hat and parabolic jet velocity profiles.

This second part contains the quantitative result of a detailed parametric study to explore the (Re, h/δ) dependence for top hat and parabolic exit velocity profiles. We arrive at a very similar formula as that of Brown (1937) on a much broader experimental and computational basis. Moreover, it is also shown that the phase of the jet disturbance between the nozzle and the wedge does not vary linearly with the distance from the nozzle, thus the convection velocity of the jet disturbance is not constant, as usually assumed in the theoretical models.

Keywords

Edge tone

István Vaik
Roxána Varga
Department of Hydrodynamic Systems,
Budapest University of Technology and Economics
György Paál
Department of Hydrodynamic Systems,
Budapest University of Technology and Economics
e-mail: paal@hds.bme.hu

1 The Reynolds number and dimensionless nozzle-to-wedge *h/δ* dependence of the Strouhal number

1.1 Reynolds number dependence of the Strouhal number (at *h/δ* ≈ 10)

Within each stage the frequency of oscillation (f) was found to be a linear function of the (mean) exit velocity of the jet (u) in both the top hat and the parabolic cases:

$$f \approx a_1 + a_2 \cdot u \tag{1}$$

Thus the Strouhal number (based on f, the δ width of the jet and u as: $St = f\delta/u$) of each stage is:

$$St(Re) = \frac{a_1 \cdot \delta}{u} + a_2 \cdot \delta = \frac{a_1 \cdot \delta^2 / \nu}{u \cdot \delta / \nu} + a_2 \cdot \delta = \frac{c}{Re} + St_\infty, \tag{2}$$

where Re is the Reynolds number based on u, δ and the kinematic viscosity of the air (ν): $Re = u\delta/\nu$. The values of c and St_∞ for the different stages deduced by the method of least squares from the results of the experiments and from the CFD simulations are collected in Table 1 for all the three stages in both of the cases (separating the results of the pure first stage oscillation and the results of the first stage of a multi stage coexistence mode).

Figure 1 summarises the results of the computational and experimental investigations in the top hat case. The Strouhal numbers are plotted against the Reynolds numbers for the three stages of the edge tone with a top hat jet. Brown's semi-empirical formulae are also plotted in the figure. No error bars are plotted here to avoid overcrowding the figure.

Because of the negative c values the first term of the Strouhal number (c/Re) is negative and hyperbolically tends to zero as Re grows. Thus as presented in Figure 1, the Strouhal numbers of the stages first increase in the low Reynolds number region, then they are nearly constant. Although in some cases the values of c for the CFD and for the experimental results differ significantly, the difference in the Strouhal numbers is within accuracy as seen in Figure 1. This can be because the denominator (Re) of the first term is at least an order of magnitude larger than the difference in the values of c. The difference of St_∞ is

Tab. 1. Coefficients of equation (2) for the top hat edge tone

	Stage I				Stage II		Stage III	
	c		St_∞					
	pure	multi	pure	multi	c	St_∞	c	St_∞
CFD, top hat	–0.7387	–1.079	0.04010	0.03541	–4.072	0.1034	–13.76	0.1740
Exp., top hat	–1.150	–0.6008	0.04522	0.03775	–1.800	0.1001	–1.841	0.1608
CFD, parabolic	–0.7894		0.04740		–3.094	0.1194	-	-
Exp., parabolic	–1.169	–0.6269	0.05070	0.04435	–3.012	0.1320	13.52	0.1854

also significant in the pure first stage mode but there Re is in the range of 60 – 250, thus c/Re is a non-negligible part of the Strouhal number.

The Reynolds number dependence of the Strouhal number in the parabolic case is not presented graphically here but can be found in e.g. [8]. In the parabolic case – contrary to the top hat case – the value of c is not negative for all the stages. Although in the experiments it was found that c is positive for the third stage, the first term (c/Re) of equation (2) is in this case at least two orders of magnitude smaller than the second term, thus it practically means that the Strouhal number is constant.

In the case of CFD simulations the results of the first stage were not separated to "pure" and "multi" parts because the first stage disappeared too early, and first and second stage multi-stage coexistences were experienced only in a few cases. Therefore the curve fitted to these points are between the curves of the experimental results for the pure first stage and the first stage of a multi-stage coexistence modes.

1.2 h/δ dependence of the Strouhal number (at fixed Reynolds numbers)

The results of all of the numerical and experimental investigations at different Reynolds numbers show that the frequency of oscillation is a linear function of $1/h$, in both the top hat and the parabolic cases.

$$f \approx b_1 \cdot \frac{1}{h} + b_2 \tag{3}$$

Thus the Strouhal number (at a fixed Reynolds number):

$$St\left(\frac{h}{\delta}\right) = \frac{b_1 \cdot \delta}{h \cdot u} + \frac{b_2 \cdot \delta}{u} = d \cdot \frac{1}{h/\delta} + St_* \tag{4}$$

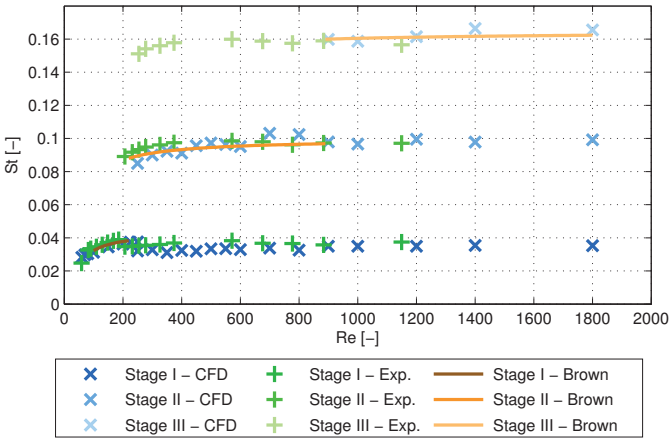

Fig. 1. Reynolds number dependence of the Strouhal number; top hat profile, $h/\delta \approx 10$

Values of d and St_* (deduced by the method of least squares) are presented in Table 2 for the results of the top hat case with $Re = 350$ (CFD simulations) and $Re \approx 350$ (experiments). Results are only presented in these two cases as the results of the other cases (at different Reynolds numbers and/or with parabolic profiles) are similar to this and the aim of this subsection is to show the linear dependence of the Strouhal number on the reciprocal of the dimensionless nozzle-to-wedge distance and the agreement between the CFD simulations and the experiments. Figures with the h/δ dependence of the Strouhal numbers at other Reynolds numbers will be shown later in Figures 3 and 4 in the next subsection with an universal St (Re, h/δ) function that fits all the results of the top hat or the parabolic cases.

The value of St_* is not negligible as it is about 5 – 10% of the first term at $h/\delta = 10$. This somewhat explains the uncertainty

Tab. 2. Coefficients of equation (4) for the top hat edge tone at $Re = 350$ for the CFD simulations and $Re \approx 380$ for the measurements

	Stage I				Stage II		Stage III	
	pure		multi					
	d	St_*	d	St_*	d	St_*	d	St_*
CFD	0.4079	0.002681	0.4288	–0.003141	0.9174	–0.000980	-	-
Exp.	0.4259	0.003732	0.4080	–0.004638	0.9975	–0.003446	1.755	–0.01815

about the value of k described in the Introduction (first part of the publication). A pure

$$\frac{d}{h/\delta}$$

function is not sufficient to achieve a perfect fit for St. In the case of a negative St_* value if a pure inverse proportional function fits well the Strouhal numbers at medium h/δ values then it underestimates the Strouhal numbers at lower h/δ and overestimates the Strouhal numbers at higher h/δ values. This can be somewhat balanced if the exponent of h/δ in the denominator is higher than 1.

Figure 2 shows the third stage of the edge tone in the measurements at $Re \approx 380$ with three fitted curves. Although all the three curves are within the measurement accuracy it can still be observed, that the red one (that has the linear formula presented in equation (4)) follows best the trend of the measured points. While the green curve – that has a form of $d/(h/\delta)^k$ with $k = 1$ – over/underestimates at the two ends of the dataset with approximately 3% while this is somewhat corrected with $k = 1.22$ (the value suggested by Jones [4]– blue curve).

1.3 *St* (*Re*, *h/δ*)

It was found that the frequency of oscillation at a fixed geometry (fixed h value) is a linear function of the mean exit velocity of the jet (u) (equation (1)) and at a fixed u is a linear function of $1/h$ (equation (3)). These suggest that the frequency is a bilinear function of u and $1/h$. It was found that instead of the most general bilinear form with four parameters:

$$f(u,h) = q_1 + q_2 \cdot u + q_3 \cdot \frac{1}{h} \cdot q_4 \cdot u \cdot \frac{1}{h})$$

the following somewhat more specific form also fits perfectly with only three parameters:

$$f(u,h) = p_1 (u + p_2)\left(\frac{1}{h} + p_3\right) \tag{5}$$

Calculating the Strouhal number:

$$St(u,h) = \frac{f \cdot \delta}{u} = p_1\left(1 + \frac{p_2}{u}\right)\left(\frac{1}{h/\delta} + p_3 \cdot \delta\right) = \\ = \left(p_1 + \frac{p_1 \cdot p_2 \cdot \delta / \nu}{u \cdot \delta / \nu}\right)\left(\frac{1}{h/\delta} + p_3 \cdot \delta\right) \tag{6}$$

This formula has the same form as that suggested by Brown [2] or by Brackenridge [1].

Because of similarity rules, if the width of the slit on the nozzle changes but the dimensionless nozzle-to-wedge distance and the Reynolds number are the same, the flow should behave similarly, i.e. the Strouhal number should be the same. This was verified by CFD simulations with an increased jet width ($\delta = 3.2$ mm) but same dimensionless nozzle-to-wedge distance ($h/\delta = 10$) at a few Reynolds numbers ($Re = 150$, 200, 250 and 300). The Strouhal numbers of these simulations are collected in Table 3 together with the Strouhal numbers at these Reynolds numbers of the $\delta = 1$ mm case. It was found that the second stage sets in at the same Reynolds number and the Strouhal numbers agree well.

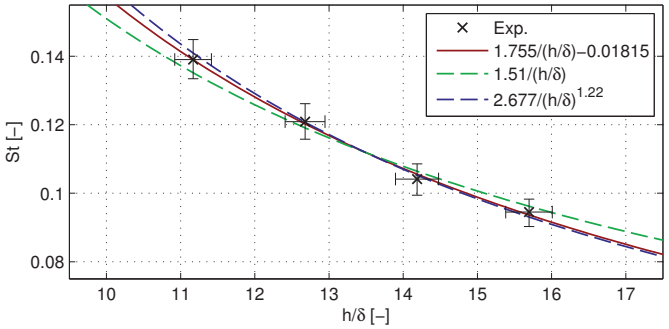

Fig. 2. Strouhal numbers of the third stage top hat edge tone at $Re \approx 380$ and $h/\delta \approx 11 - 16$; Best fit curves of type $d/(h/\delta)^k$, k = 1, 1.22 and $d/(h/\delta) + St_*$ are plotted for comparison

Therefore, as long as the dimensionless nozzle-to-wedge distance is kept constant the width of the slit on the nozzle itself should not have any influence on the Strouhal number of the stages of the edge tone, thus the Strouhal number can be written as the following:

$$St\left(Re, \frac{h}{\delta}\right) = \left(c_1 - \frac{c_2}{Re}\right)\left(\frac{1}{h/\delta} - c_3\right) \tag{7}$$

The results of the computational and the experimental investigations differ within their accuracies therefore curve fitting was carried out on the joint dataset. In these cases the built-in nonlinear least square method of MatLab was used for the curve fitting. Table 4 shows the coefficients of the best fit curves together with the coefficient of determination (R^2 value) of the fit. (The coefficient of determination of a $y = f(x)$ function fitted onto a set of x_i, y_i $i = 1, \ldots, n$ values is a measure for the quality of the fit. It is defined as

$$R^2 = 1 - \frac{\sum_{i=1}^{n}\left(y_i - f(x_i)\right)}{\sum_{i=1}^{n}\left(y_i - \bar{y}\right)^2}, \text{ where } \bar{y} = \frac{1}{n}\sum_{i=1}^{n} y_i.)$$

Tab. 3. Strouhal numbers of the edge tone with nozzles that have δ = 1 mm or δ = 3.2 mm wide slit on them but having geometric configuration with the same $h/\delta = 10$ dimensionless nozzle-to-wedge distance

Re [-]	St [-]			
	δ = 1 mm		**δ = 3.2 mm**	
	Stage I	Stage II	Stage I	Stage II
150	0.0345	-	0.0345	-
200	0.0362	-	0.0352	-
250	0.0375	0.0849	0.0369	0.0856
300	0.0328	0.0900	0.0361	0.0901

Its value – except for the first stage of the multi-stage mode case – is always higher than 0.95 thus the fit is good enough. Even in that case it is still not lower than 0.9, thus acceptable. In this case the rms value of the relative difference between the measured Strouhal numbers and the fitted curve is about 6%, and can be explained as a consequence of the difference between the Strouhal numbers of the experiments and the CFD simulations found during the Reynolds number dependence study that is in all other cases much lower.

Brown used the same $c_3 = 0.007$ parameter for all the three stages, while in our case it varies from stage to stage. The values of the parameters of the pure first and the second stages agree well (Brown did not publish results for the first stage of a multi stage mode). Although the values for the third stage seem to be a bit different, if it is kept in mind that Brown observed the third stage Reynolds numbers above 900, then it can be concluded that the c_2/Re part is almost negligible compared to c_1 and the difference in c_3 compensates the difference in c_1. At $h/\delta = 10$ both Brown's and our formula gives 0.1646 if the c_2/Re part is neglected.

In the case of the fourth stage of the parabolic edge tone, the three parameters of the curve are determined from only four observations, therefore – although it fits the results – it should be treated with caution. This also explains the qualitative difference of this case compared to the other cases (i.e. only in this single case c_2 is negative).

Tab. 4. Coefficients of St (Re, h/δ) formula – equation (7)

		c_1 [-]	c_2 [-]	c_3 [-]	R^2
Top hat	Stage I pure	0.4837	12.31	0.005461	0.9941
	Stage I multi	0.4167	0.2292	0.01426	0.9015
	Stage II	1.066	27.11	0.004157	0.9614
	Stage III	1.884	19.96	001261	0.9934
Brown [2]	Stage I	0.4659	12.06	0.007	
	Stage II	1.072	27.74	0.007	
	Stage III	1.77	45.83	0.007	
Parabolic	Stage I pure	0.5230	11.08	0.004836	0.9953
	Stage I multi	0.5029	6.6451	0.01417	0.9832
	Stage II	1.177	37.15	–0.002273	0.9786
	Stage III	1.972	6.954	0.007792	0.9916
	Stage IV	2.365	–55.21	–0.000999	0.9982

Figures 3 and 4 show the values of the Strouhal number from the CFD and the experimental investigations together with the fitted curves in the top hat and in the parabolic cases, respectively.

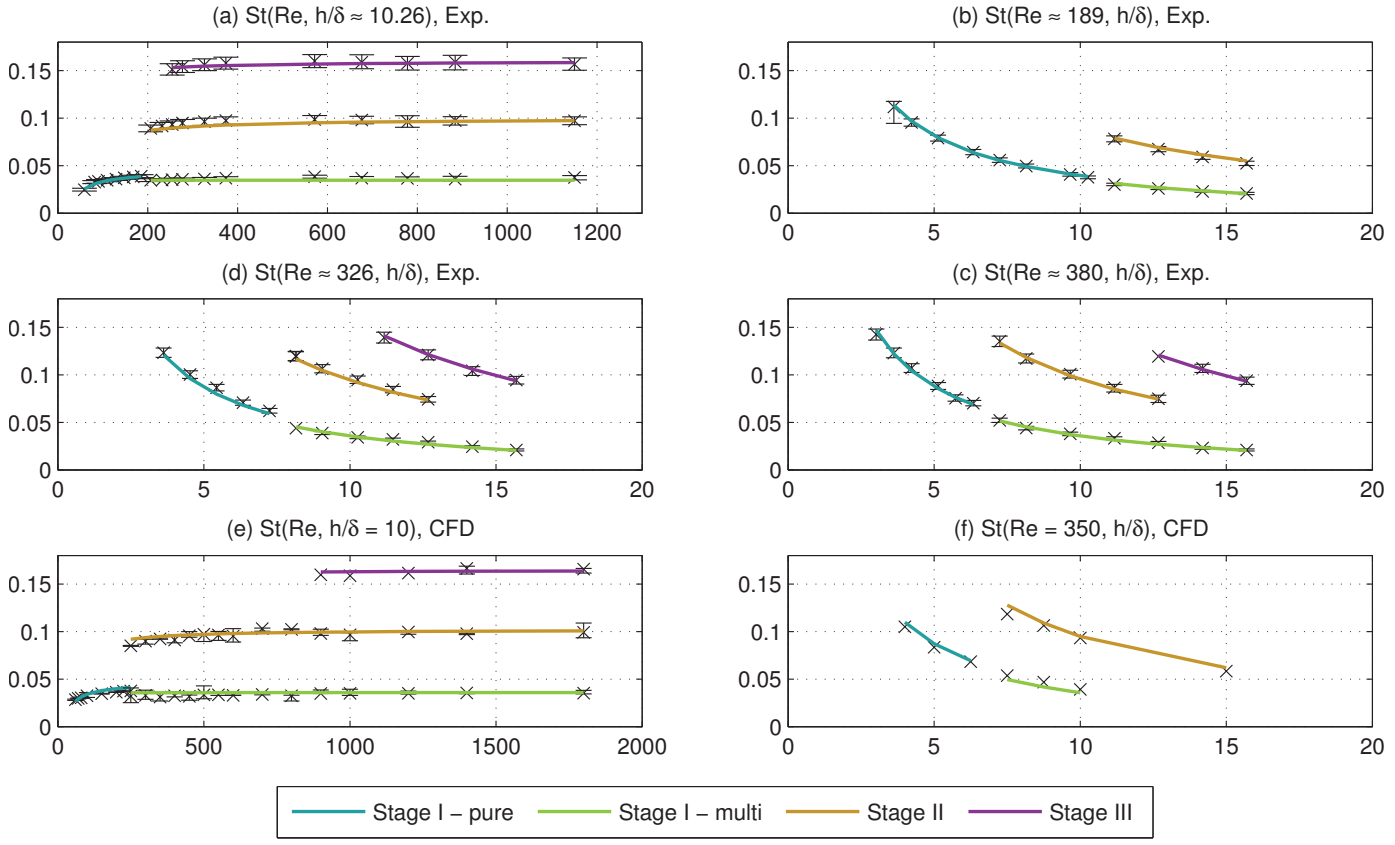

Fig. 3. Strouhal numbers of the top hat edge tone. Crosses with error bars denote the numerical (CFD) or experimental (Exp.) results. Solid lines are the best fit curves described in equation (7) with coefficients in Table 4

2 Convection velocity and wavelength of the disturbance

The previous sections showed that the experimental and computational results agree well, thereby validating the results of the CFD simulations. Thus further detailed investigation of the flow can be carried out with the help of these simulations: e.g. the pressure distribution on the wedge wall or the phase of the propagating disturbance between the nozzle and the wedge can be easily and cost-effectively investigated.

It is crucial in the understanding of the exact mechanism of the edge tone oscillation to determine the velocity of the disturbance propagation along the jet. In the literature a theoretical value of 0.5 times the mean exit velocity is given [6]. The theory is with an assumption of an inviscid parallel jet and corresponds to the phase velocity of the most unstable frequency disturbance. Experimental values scatter around 0.5 times the mean exit velocity (e.g. Curle [3] found values around 0.3 – 0.6, Brown [2] reported values around 0.4, Kwon [5] found 0.5 – 0.6). The expression "phase velocity" is meaningful only if there is only one pure sinusoidal disturbance present or if the system is non-dispersive; when several modes are superposed on each other, each mode propagates with a different velocity or the various modes may interact with each other in an unknown way. In a multi-stage operation a disturbance convection velocity can be identified as a group velocity rather then a phase velocity; or, alternatively the phase velocity can be determined for each mode separately. Here only the pure first stage case will be considered.

The convection velocity of the disturbance was determined with a cross-correlation technique. The instantaneous transversal component of the velocity at several points between the nozzle and the wedge tip was compared to one of them chosen as the reference point (usually approximately at $0.6h$). The signal of the first point was shifted by i time steps, and then the correlation coefficient (R) between the shifted signal of the first point and the reference signal was calculated. The phase delay (relative to the reference point) is determined as

$$\phi = i_{\max} \cdot \Delta t \cdot \frac{2\pi}{T},$$

where i_{max} is the shift value where R reaches its maximum, Δt is the time step of the two signals and T is the period time. Figure 5 shows the transversal component of the velocity at the reference point (blue line) and at a distance $0.25 \cdot h$ away from the nozzle (red line). The dashed red line corresponds to the latter signal shifted by the time lag (determined as described above) between the two signals.

Figure 6 shows the phase delay divided by

$$2\pi\left(\phi_* = \frac{\phi}{2\pi}\right).$$

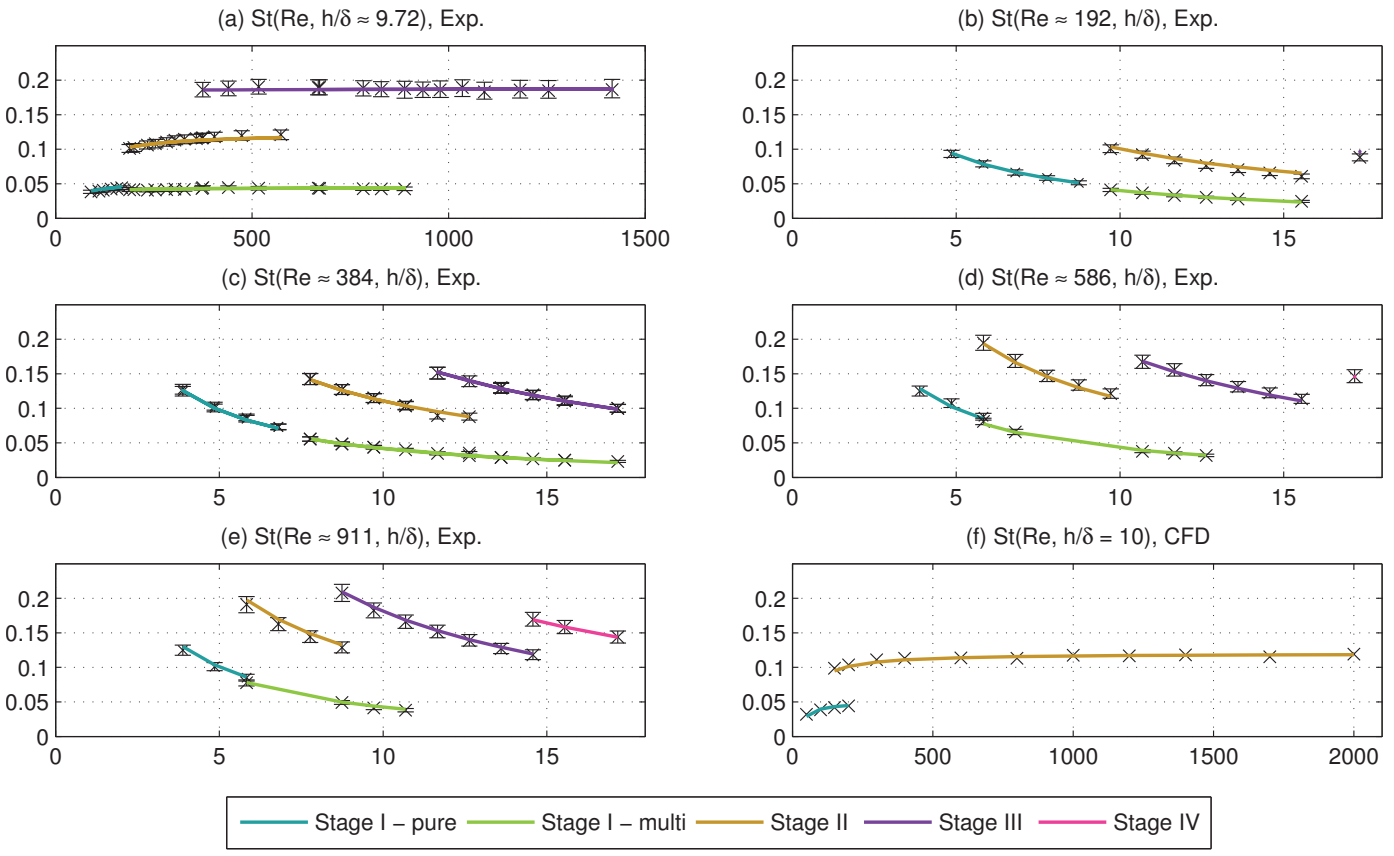

Fig. 4. Strouhal numbers of the parabolic edge tone. Crosses with error bars denote the numerical (CFD) or experimental (Exp.) results. Solid lines are the best fit curves described in equation (7) with coefficients in Table 4

The absolute numbers on the vertical axis are not important thus the starting point of the curve was adjusted to 0. It became apparent that this curve is universal in the sense that it applies for every first stage single-mode Reynolds number (only results of simulations with $h = 10$ mm were used for this investigation). The phase delay is parabolic, the fitted functions differ negligibly in the case of different Reynolds numbers. Fitting a parabola to all the points together results in:

$$\phi_*\left(\frac{x}{h}\right) = \frac{\phi\left(\frac{x}{h}\right)}{2\pi} \approx 0.6036 \cdot \left(\frac{x}{h}\right)^2 + 0.2781 \cdot \frac{x}{h} \tag{8}$$

This agrees almost perfectly with the power function

$$\frac{\phi}{2\pi} = 0.9 \cdot \left(\frac{x}{h}\right)^{1.63}$$

suggested by Stegen and Karamcheti [7] after measuring the phase at $Re \approx 950$ and $h/\delta \approx 5.58$. Figure 6 shows the two curves together with the result of the CFD simulations at $Re = 950$, $h/\delta = 10$ with a top hat jet.

In the nozzle-to-wedge distance the phase drops by almost a full period. The acoustic wave of the dipole sound source that excites the jet and generates the next instability wave reaches the nozzle immediately, therefore the fact that the phase drop does not reach a full period in the nozzle-to-wedge distance means that the effective dipole sound source is somewhat behind the tip of the wedge.

The derivative of the inverse function of $T \cdot \phi_*$ (where T is the period) multiplied by h yields the phase velocity that is actually the convection velocity of the disturbance:

$$u_{con} = \frac{h}{T \cdot \phi_*'} \tag{9}$$

Thus, its relative value follows as:

$$\frac{u_{con}}{u} = \frac{h}{T \cdot u} \cdot \frac{1}{\phi_*'} = St \cdot \frac{h}{\delta} \cdot \frac{1}{\phi_*'} \tag{10}$$

Only first stage edge tone oscillations with $h/\delta = 10$ were simulated but both with top hat and parabolic profiles. The former one results in Strouhal numbers from 0.028 to 0.044 while the latter from 0.032 to 0.044 . Therefore the relative values of the convection velocities are very high (1 – 1.58) at the orifice and they continuously and rapidly decrease further downstream to values of 0.19 – 0.3. The initially high disturbance convection velocities can be explained so that the disturbances have not developed there yet – instead the jet moves rather like a "solid stick". Since there is a continuous change of the convection velocity it makes no sense to talk about "wavelength" because within one wavelength the "wavelength" changes. The average relative convection velocity values are between 0.32 – 0.41 and 0.43 – 0.5 in the top hat and parabolic cases, respectively. These agree well with the values found by

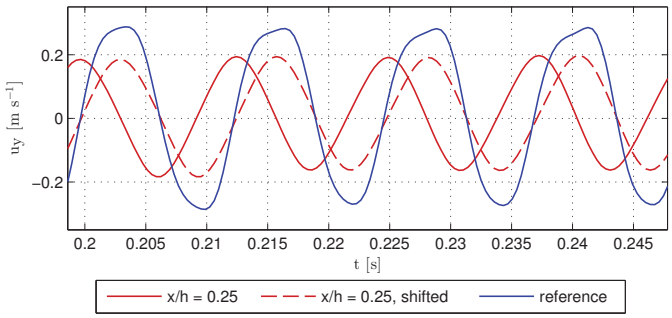

Fig. 5. Transversal velocity signals used for the cross correlation of a top hat edge tone flow with $Re = 150$ and $h/\delta = 10$

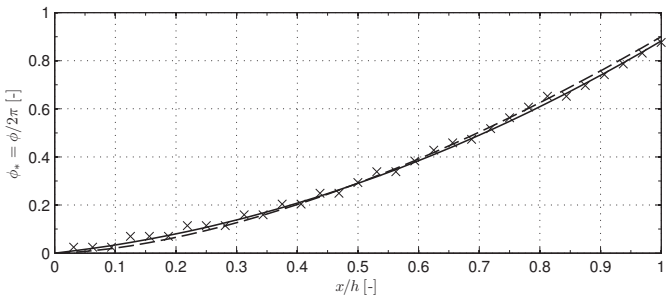

Fig. 6. Phase drop of a first stage edge tone oscillation; Results from CFD simulation at $Re = 200$ and $h/\delta = 10$, top hat profile (X); Fitted parabola (equation (8), solid line) and power function suggested by Stegen and Karamcheti [7] (dashed line)

Brown [2] but are also not far from the theoretical value of Mattingly and Criminale [6].

3 A possible reason for the differences between results with parabolic and top hat profiles

As shown in the first part of the publication in the case of parabolic edge tones the Strouhal number is about 15 – 20% larger relative to the top hat edge tones at the same Reynolds numbers, i.e. at the same mean exit velocity values, i.e. at equal mass flow rates.

The momentum and the energy that is injected to the system is proportional to

$$\int_{-\delta/2}^{\delta/2} u(y)^2\, dy \text{ and } \int_{-\delta/2}^{\delta/2} u(y)^3\, dy,$$

respectively. Therefore if the Reynolds number were based on the quadratic mean value

$$\left(\text{qmv},\ u_{qmv} = \sqrt{\frac{1}{\delta}\int_{-\delta/2}^{\delta/2} u(y)^2\, dy}\right)$$

or the cubic mean value

$$\left(\text{cmv},\ u_{cmv} = \sqrt[3]{\frac{1}{\delta}\int_{-\delta/2}^{\delta/2} u(y)^3\, dy}\right)$$

of the inlet velocity instead of the average (mean) velocity

$$\left(\text{avr},\ u_{avr} = \frac{1}{\delta}\int_{-\delta/2}^{\delta/2} u(y)\,dy\right),$$

the same amount of momentum or energy would be injected into the system at the same Reynolds number independently of the velocity profile.

The qmv of the

$$u(y) = \frac{3}{2}\overline{u}\left(\frac{\delta^2}{4} - y^2\right)\frac{4}{\delta^2}$$

parabolic profile – that has an average velocity of $\overline{u}$ – is $u_{qmv} \approx 1.095 \cdot \overline{u}$ therefore if based on that, compared to the conventional definition, the Reynolds number would increase by a factor 1.095 and the Strouhal number would decrease by a factor of 1.095. The cmv of the same parabolic profile is $u_{cmv} \approx 1.156 \cdot \overline{u}$, therefore using that the Reynolds number would increase by a factor 1.156 and the Strouhal number would decrease by a factor of 1.156.

Figure 7 shows the Reynolds number dependence of the Strouhal numbers when the mean velocity, the qmv or the cmv are used for the Reynolds and Strouhal numbers. Further investigations are needed to explore the reasons but it can still be noted that for low Reynolds numbers it seems that using the quadratic mean value for the Reynolds and Strouhal numbers gives a better agreement in the Strouhal numbers of top hat and parabolic edge tones; and for higher Reynolds numbers it seems that using the cubic mean value for the Reynolds and Strouhal numbers gives a better agreement in the Strouhal numbers of top hat and parabolic edge tones. These would indicate the importance of the momentum/energy flow rate equivalence, rather than the mass flow rate equivalence.

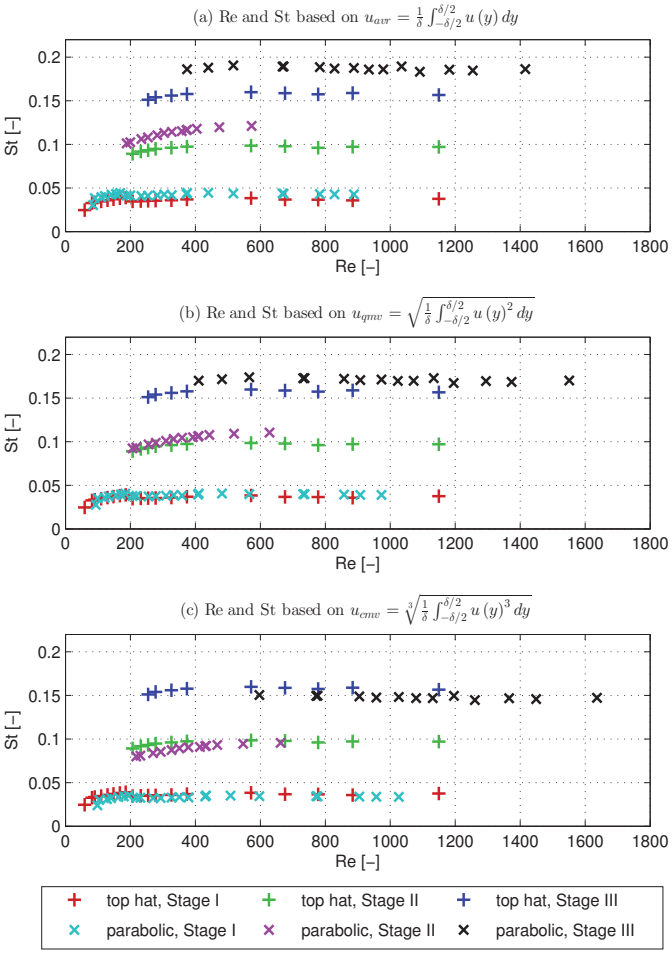

Fig. 7. Influence of the velocity averaging on the Strouhal number – Reynolds number relationship

4 Summary

The flow of the edge tone has been investigated both by numerical and experimental means. The planar nature of the flow was verified by comparing the results of the 2D and the 3D CFD simulations and also experimentally by flow visualization. Parametric studies were carried out to determine how the Strouhal number of the oscillation depends on the Reynolds number and on the dimensionless nozzle-to-wedge distance. The results of the CFD simulations agree well with those of the experiments, the formulae describing the St (Re, h/δ) relationships in case of top hat and parabolic edge tones were determined. These formulae are very close to that of Brown [2] but are based on a more thorough reasoning. In the case of the top hat exit velocity profile the numerical values of the parameters are also very close to those of Brown [2]. Moreover, the phase and convection velocity of the jet disturbance was investigated, and it was found that the phase varies nonlinearly with the distance from the nozzle, thus the convection velocity is not constant as it is assumed in all of the theoretical considerations. The work presented here also verifies that the edge tone phenomenon can be reliably simulated with a commercial CFD code, thus opening the possibility to numerically investigate more complex, real life occurrence of self-sustained flow oscillations such as the flow in the foot of an organ pipe.

References

1 **Brackenridge J. B.,** *Transverse Oscillations of a Liquid Jet. I.* The Journal of the Acoustical Society of America, 32(4), 1237-1242 (1960). DOI: 10.1121/1.1907888

2 **Brown G. B.,** *The vortex motion causing edge tones*. Proceedings of the Physical Society, 49(5), 493-507 (1937). DOI: 10.1088/0959-5309/49/5/306

3 **Curle N.,** *The mechanics of edge-tones*. Proceedings of the Royal Society A, 216(1126), 412-424 (1953). DOI: 10.1098/rspa.1953.0030

4 **Jones A. T.,** *Edge Tones*. The Journal of the Acoustical Society of America, 14(2), 131-139 (1942). DOI: 10.1121/1.1916208

5 **Kwon Y.-P.**, *Phase-locking condition in the feedback loop of low-speed edgetones*. The Journal of the Acoustical Society of America, 100(5), 3028-3032 (1996).
DOI: 10.1121/1.417114

6 **Mattingly G. E.**, *Criminale W. O., Disturbance Characteristics in a Plane Jet*. Physics of Fluids, 14(11), 2258-2264 (1971).
DOI: 10.1063/1.1693326

7 **Stegen G. R., Karamcheti K.**, *Multiple tone operation of edgetones*. Journal of Sound and Vibration, 12(3), 281-284 (1970).
DOI: 10.1016/0022-460X(70)90072-6

8 **Vaik I., Paál G.**, *Mode switching and hysteresis in the edge tone*. Journal of Physics: Conferece Series, 268(1), No. 012031, (2011).
DOI: 10.1088/1742-6596/268/1/012031